Chemical Physics Letters 573 (2013) 84–89

Contents lists available at SciVerse ScienceDirect

Chemical Physics Letters

journal homepage: www.elsevier.com/locate/cplett

Direct diabatization of electronic states by the fourfold-way: Including dynamical correlation by multi-configuration quasidegenerate perturbation theory with complete active space self-consistent-field diabatic molecular orbitals

Ke R. Yang, Xuefei Xu, Donald G. Truhlar *

Department of Chemistry, Chemical Theory Center, and Supercomputing Institute, University of Minnesota, Minneapolis, MN 55455-0431, USA

ARTICLE INFO

Article history:
Received 13 January 2013
In final form 16 April 2013
Available online 23 April 2013

ABSTRACT

We propose a new scheme for the direct diabatization of MC-QDPT wave functions. Our new scheme utilizes CASSCF diabatic molecular orbitals (DMOs); this is conceptually simpler than the previous approach and can lead to smoother diabatic potentials. We validated the new diabatization scheme, in comparison to CASSCF diabatization and to the original MC-QDPT diabatization scheme, for two test cases, the dissociation of LiF and the reaction of Li + FH → LiF + H. The results with our new scheme suggest that the new scheme with CASSCF DMOs would be a good choice for nonadiabatic dynamics studies in the future.

1. Introduction

The widely used Born–Oppenheimer (BO) approximation separates the electronic and nuclear motions, which leads to the concepts of adiabatic states and potential energy surfaces (PESs). Adiabatic PESs are associated with adiabatic electronic states, which are the eigenstates of the electronic Hamiltonian at each nuclear configuration. The couplings between nuclear motions and electronic motions are usually called nonadiabatic coupling. In the adiabatic representation, nonadiabatic couplings are off-diagonal matrix elements of the nuclear momentum vector and the nuclear kinetic energy, although the latter is often neglected in semiclassical treatments [1]. The former are $(3N_A - 6)$-dimensional vectors, where N_A is the number of atoms in the molecule. The couplings can be rapidly varying in avoided crossing regions where two or more adiabatic PESs approach closely, and they are singular along $(3N_A - 8)$-dimensional conical intersection seams; this makes them inconvenient for dynamical studies of photodissociation, predissociation, quenching of excited states in collisions, chemiluminescence, etc. The use of diabatic representations [2] has been proposed as an alternative approach to study dynamics. In nonadiabatic representations (any representation except the adiabatic one), the states are coupled not only by the nuclear momentum and kinetic energy but also by the electronic Hamiltonian; diabatic states are nonadiabatic states whose momentum and kinetic energy couplings are negligible compared to the electronic Hamiltonian couplings, which are off-diagonal elements of the electronic Hamiltonian matrix. The electronic Hamiltonian couplings are slowly varying, nonsingular scalars and hence are much more convenient for dynamical calculations. Strictly diabatic states would be states whose nuclear momentum and kinetic energy couplings (nonadiabatic couplings) vanish completely and globally; they do not exist in general [3], so one has to develop methods to obtain diabatic states whose nonadiabatic couplings are negligible but not strictly vanishing.

Many methods, based on a variety of criteria, have been proposed to calculate diabatic states, which are not unique, and they are briefly discussed in Refs. [4,5] (with more than 50 references to previous treatments). Among these methods, the fourfold-way diabatization scheme [4–6] proposed by Nakamura and one of the authors is very promising and has been applied to study of the photodissociation of ammonia [7–10], bromoacetyl chloride [11], hydrogen bromide [12], and chlorobromomethane [13]. One important advantage of the fourfold-way over alternative schemes is that it is 'direct', which in this context means that the diabatic potentials and couplings calculated at a given geometry are independent of any path leading to that geometry. Another important feature of fourfold-way diabatization is that one obtains N diabatic electronic states that span the same space as N chosen adiabatic states (for example, the N lowest).

The fourfold-way algorithm is based on the density matrix, and it was originally proposed [4] for the diabatization of complete-active-space (CAS) self-consistent-field (CASSCF) [14–16] wave functions. However, CASSCF is not quantitatively accurate because it includes only a small fraction of the dynamical correlation. To include dynamical correlation, the method was further developed

* Corresponding author. Fax: +1 612 626 9390.
E-mail addresses: yang1466@umn.edu (K.R. Yang), xuxuefei@gmail.com (X. Xu), truhlar@umn.edu (D.G. Truhlar).

0009-2614/$ - see front matter © 2013 Published by Elsevier B.V.
http://dx.doi.org/10.1016/j.cplett.2013.04.036

for the diabatization of multi-configuration quasi-degenerate perturbation theory (MC-QDPT) [17,18], which (like multi-state CASPT2 [19]) is a 'perturb, then diagonalize' effective Hamiltonian variant of the multi-reference perturbation theory (MRPT) [20–23]. In this Letter, we present a simpler scheme to perform diabatization of MC-QDPT wave functions, and we test its performance for two test cases, namely, the dissociation of LiF and the reaction Li + FH → LiF + H.

In order to obtain diabatic states, the multi-electron wave functions are expressed in terms of diabatic molecular orbitals (DMOs) rather than the usual canonical molecular orbitals (CMOs) because the DMOs vary smoothly with geometry, whereas the CMOs need not be smooth along continuous nuclear-coordinate paths. In the original algorithms, the CASSCF diabatic states were expressed in terms of DMOs obtained from the CASSCF wave function, and the MC-QDPT diabatic states were expressed in terms of DMOs obtained using a density matrix based on the eigenvectors of the MC-QDPT effective Hamiltonian. In the algorithm presented here, the MC-QDPT diabatic states are expressed in terms of the CASSCF DMOs; this simplifies the treatment and, more importantly, it was motivated by our observation that the CASSCF DMOs are sometimes smoother than the DMOs that result from the more complicated MC-QDPT procedure. The quality of the diabatic states is not compromised by using the CASSCF DMOs because the new diabatic states still span the same space as the N MC-QDPT adiabatic states that they replace.

We stress that the goal of the diabatization scheme considered here is to obtain a set of diabatic states that span the same space as a chosen set of adiabatic states, but for which the coupling by the nuclear momentum operator is negligible compared to the effect of coupling by the electronic Hamiltonian. This will allow convenient treatments of electronically nonadiabatic states. (Since nonadiabatic states are not unique, some other workers have defined them with other objectives in mind, for example [24] to account for electron–nuclear correlation.) Because the diabatic states span the same space as the adiabatic ones, the method is not designed to overcome any limitations in the method used to obtain adiabatic states. For example, if or when the MC-QDPT method makes significant errors due to an incomplete treatment of electron correlation or gives nonsmooth adiabatic potential curves near places where the CASSCF states cross, the diabatization scheme does not correct these problems. But it does provide a convenient way to carry out dynamics at the MC-QDPT level, and this level (which is essentially the same as multistate CASPT2) has been demonstrated to provide useful accuracy for studying many photochemical processes. Nevertheless, it would be useful in future work to apply this diabatization scheme to other methods for calculating sets of ground and excited state potential energy surfaces, such as extended multi-configuration quasi-degenerate perturbation theory [25] (XMC-QDPT) or extended multi-state complete active space second-order perturbation theory [26] (XMS-CASPT2), which would be expected to produce smoother adiabatic curves near surfaces crossings, or even to more significantly different methods such as multireference configuration interaction [27–29]. The present simplification of the method such that the DMOs are determined at the CASSCF level will facilitate such extensions.

2. Theory

The fourfold-way diabatization scheme is limited (at the present time) to complete active space methods (e.g., CASSCF, CASPT2, and MC-QDPT based on a CASSCF reference). In CAS methods, the molecular orbitals are divided into three classes: inactive orbitals that are doubly occupied in all reference configurations, external orbitals that are unoccupied in all reference configurations, and active orbitals that have variable occupation (0, 1, or 2) in reference configuration state functions (CSFs). The limitation to CAS methods is because we take advantage of the invariance of CASSCF wave functions to orbital rotations that do not mix orbitals from the different classes, in particular transformations that mix the active orbitals among themselves.

We will briefly discuss the fourfold-way diabatization method and then present our new scheme for diabatization of MC-QDPT wave functions with CASSCF DMOs. For more details of the original scheme, please refer to the original fourfold-way diabatization papers [4,5].

2.1. The original fourfold-way algorithms for diabatization

We obtain N diabatic states ϕ_k, with $k = 1 \ldots N$, by orthogonal transformation (assuming all wave functions are real) of the N adiabatic states ψ_n, with $n = 1 \ldots N$, as follows

$$\phi_k = \sum_{n=1}^{N} \psi_n T_{nk} \tag{1}$$

where T_{nk} is an element of the orthogonal adiabatic-to-diabatic transformation matrix **T**. The adiabatic states are linear combinations of L orthonormal CSFs, χ_α,

$$\psi_n = \sum_{\alpha=1}^{L} c_{\alpha n} \chi_\alpha \tag{2}$$

where the coefficients $c_{\alpha n}$ are obtained variationally or by perturbation methods. We consider systems for which each adiabatic state is dominated by a small set of CSFs at potential reference geometries, which are geometries where adiabatic states are almost equal to diabatic states. At potential reference geometries, one can identify 'dominant' CSFs, χ_δ (called diabatic prototypes), that make large contributions to one and only one of the N adiabatic states of interest, and one can divide them into N groups as follows:

Group G_1: $\{\chi_\delta\}$, $\delta = 1 \ldots a_1$, which are mainly important for ψ_1;
Group G_k: $\{\chi_\delta\}$, $\delta = (a_{k-1} + 1) \ldots a_k$, which are mainly important for ψ_k;
Group G_N: $\{\chi_\delta\}$, $\delta = (a_{N-1} + 1) \ldots (a_N = M)$, which are mainly important for ψ_N.

where M is the total number of diabatic prototypes in all of the groups. The dominant CSF group lists G_k (with $k = 1 \ldots N$) may be used to form templates of the diabatic states ϕ_k, $k = 1 \ldots N$, provided that we exclude any CSF that would be prominent in more than one diabatic state as we vary the geometry. One may need to consider more than one potential reference geometry and make dominant CSF lists by taking the union of the dominant CSF lists at each of them. Furthermore, sometimes one needs to add diabatic prototypes to the lists even when they are not identified at potential reference geometries.

At any geometry, we can obtain approximate wave functions for the N adiabatic states ψ_n, with $n = 1 \ldots N$, using either CASSCF or MC-QDPT. With the predefined dominant CSF lists G_k and the calculated coefficients $c_{\alpha n}$ of the N adiabatic states ψ_n expressed in terms of these CSFs, the adiabatic/diabatic transformation matrix **T** is determined by the configuration uniformity procedure introduced by Atchity and Ruedenberg [30]. The details of the step to determine **T** are given in Refs. [4,5], and we will not change or discuss them here.

The CSFs in the group lists must be smooth functions along nuclear-coordinate paths, as required for them to fulfill their mandate as diabatic prototypes; thus the molecular orbitals (MOs) that are used to construct these dominant CSFs have to change smoothly along paths in nuclear coordinate space. These MOs that change smoothly are the DMOs we mentioned above.

The fourfold algorithm for constructing DMOs consists of the threefold density matrix criterion and the maximum overlap refer-

ence MOs (MORMO) criterion. The threefold density matrix criterion is the maximization of the functional defined as:

$$D_3 = \alpha_N D^{NO} + \alpha_R D^{ON} + \alpha_T D^{TD}, \tag{3}$$

where α_N, α_R, and α_T are predefined parameters. Here we use the standard values of 2, 1, and 0.5. The functional D^{NO} is called the natural orbital term and is defined as

$$D^{NO} = N\sum_{\mu=1}^{\eta}(\bar{p}_{\mu\mu})^2, \tag{4}$$

where η is the number of active MOs used to construct CSFs, and $\bar{\mathbf{p}}$ is the state-averaged density matrix (averaged over the N states of interest). The functional D^{ON} is called the occupation number term and is defined as

$$D^{ON} = \sum_{\mu=1}^{\eta}\sum_{n=1}^{N}(p^n_{\mu\mu})^2, \tag{5}$$

where $p^n_{\mu\mu}$ is the one-particle density matrix element of the adiabatic wave function ψ_n. The third term D^{TD} is called the transition density term and is defined as

$$D^{TD} = \frac{2}{N-1}\sum_{\mu=1}^{\eta}\sum_{m<n}^{N}(p^{mn}_{\mu\mu})^2, \tag{6}$$

where $\mathbf{p}^{mn}$ is the transition density matrix between adiabatic states ψ_m and ψ_n.

The MORMO criterion involves introducing λ reference MOs u^{ref}_τ, $\tau = 1\ldots\lambda$, and a reference orbital functional D^{RO}. For a specific geometry Q, D^{RO} is defined as [4–6]

$$D^{RO} = \sum_{\tau=1}^{\lambda}\left(\sum_{i=1}^{I}\sum_{j=1}^{I}a^{ref}_{\tau i}a_{\tau j}\langle\xi_i(Q)|\xi_j(Q)\rangle\right)^2, \tag{7}$$

where I is the number of atomic basis functions, $\xi_i(Q)$, $i = 1\ldots I$ are the normalized atomic orbitals, and $a^{ref}_{\tau i}$ and $a_{\tau j}$ are the coefficients of MO u^{ref}_τ at geometry Q_{ref} and Q, respectively.

To apply the fourfold-way to determine DMOs, one first maximizes D^{RO} by rotating all η active orbitals, and the λ rotated MOs that maximize D^{RO} are taken as the first λ DMOs. Then D_3 is maximized by orbital rotations within the remaining set of $\eta - \lambda$ active MOs to determine the remaining DMOs. After determining DMOs with the fourfold-way, those DMOs need to be ordered according to the DMOs at nearby geometries to construct consistent CSFs to obtain the adiabatic/diabatic transformation matrix $\mathbf{T}$ based on configuration uniformity. The determination of the transformation matrix $\mathbf{T}$ is explained in previous work [4,5].

The fourfold-way diabatization algorithm has been implemented for adiabatic states described by both CASSCF and MC-QDPT wave functions. For CASSCF wave functions, it is very clear that only DMOs spanning the same space of η active orbitals need to be determined by the fourfold-way, since the occupancies of inactive and external orbitals are the same in all CSFs, either doubly occupied or unoccupied. But this requires further justification for MC-QDPT wave functions. In general the adiabatic state, ψ^{MQ}_n, obtained with MC-QDPT can be written as

$$\psi^{MQ}_n = \sum_{\alpha=1}^{L_{CAS}}c_{\alpha n}\chi_\alpha \quad + \sum_{\alpha=L_{CAS}+1}^{L}c_{\alpha n}\chi_\alpha, \tag{8}$$

where L_{CAS} is the number of CSFs in the CAS configuration space, and L is the total number of CSFs. In CSFs χ_α with $\alpha = 1\ldots L_{CAS}$, all inactive and external orbitals are doubly occupied and unoccupied, respectively, as for CASSCF wave functions. But this is not the case for CSFs χ_α with $\alpha = L_{CAS}+1\ldots L$, in which the occupancies of inactive and external orbitals can differ from 2 and 0. However, if the active space is chosen large enough for a good description of all N states, one can expect that

$$\sum_{\alpha=1}^{L_{CAS}}c^2_{\alpha n} \quad >> \sum_{\alpha=L_{CAS}+1}^{L}c^2_{\alpha n}. \tag{9}$$

So we make the assumption that, even when dynamical correlation is included, only the DMOs spanning the active orbital space need to be determined, while the remaining orbitals can be taken as CMOs.

2.2. Including dynamical correlation by MC-QDPT with CASSCF DMOs

The original implementation of the fourfold-way diabatization of MC-QDPT wave functions is conceptually complicated by the use of MC-QDPT DMOs, and the smooth variation of the DMOs is dependent on smooth variation of the MC-QDPT effective Hamiltonian eigenvectors. Here we propose a simplified scheme to include dynamical correlation in diabatic states. The first steps are the same as before: we use the fourfold-way to obtain the CASSCF DMOs, and then the CASSCF wave functions are expressed in terms of CSFs constructed with CASSCF DMOs. In the previous MC-QCPT algorithm, the CASSCF DMOs are only used as initial MOs in the MC-QDPT adiabatic calculations, and we determine the final DMOs by applying the fourfold-way at the MC-QDPT level (these new DMOs are the MC-QDPT DMOs); then we express the wave function by Eq. (8) where χ_α is a CSF expressed in terms of MC-QDPT DMOs for the active space and CMOs for the inactive and virtual spaces. Finally the coefficients of Eq. (8) are used with the predefined dominant CSF lists in the configurational uniformity scheme to obtain the diabatic states.

In contrast, in the new method we skip the step to obtain MC-QDPT DMOs, and we replace Eq. (8) by

$$\psi^{MQ}_n = \sum_{\alpha=1}^{L_{CAS}}c^0_{\alpha n}\chi^0_\alpha \quad + \sum_{\alpha=L_{CAS}+1}^{L}c^0_{\alpha n}\chi^0_\alpha \tag{10}$$

where χ^0_α is a CSF expressed in terms of CASSCF DMOs for the active space and CMOs for the inactive and virtual spaces. With the predefined dominant CSF lists and the coefficients in Eq. (10), we calculate the adiabatic/diabatic transformation matrix and do the diabatization of MC-QDPT adiabatic states without the complication of MC-QDPT DMOs.

3. Applications

This section will illustrate the new diabatization scheme presented in Section 2 by applying it to two test systems, the dissociation of LiF and the reaction Li + FH → LiF + H. The two test cases are quite different, and they provide critical tests of the new method. The first case was chosen because it is a classic case [31] of a curve crossing whose location is very sensitive to dynamical correlation. In particular the curve crossing of the ionic and covalent interactions occurs at a much larger distance when dynamical correlation is fully included. This provides a severe test of the applicability of using CASSCF DMOs in a calculation with post-CASSCF dynamical correlation. The second test case was chosen because it is a multi-arrangement reaction system where the DMOs derived by the fourfold-way must change their character smoothly along a reaction pathway [4,5], which required an extension (in previous work) of the original configurational uniformity concept of Atchity and Ruedenberg [30].

All calculations were carried out with a locally modified version of the HONDOPLUS v5.2 program [32,33]. Computational details and results are given in the following two subsections.

3.1. First test case: LiF dissociation ($1\ ^1\Sigma^+$, $2\ ^1\Sigma^+$)

The two lowest $^1\Sigma^+$states of LiF exhibit an ionic–covalent diabatic curve crossing at large bond length. LiF is a good example to test a diabatization scheme since the location of its weakly avoided crossing of the adiabats is very sensitive to dynamical correlation; the location of the avoided crossing point is quite different for CASSCF and MC-QDPT wave functions. It is therefore a good check to demonstrate that our new scheme is able to give the proper location of the diabatic crossing in LiF.

The basis set we used is 6-311G(3df,3pd) [34,35] augmented by diffuse s and p functions with exponents 0.0052 (s) and 0.0097 (p) for Li and 0.089 (s) and 0.083 (p) for F. The active space contains the 2s orbital of Li and the 2p and 3p orbitals of F; this choice gives an active space with 6 electrons in 7 orbitals. The 1s orbitals of the Li and F atoms and the 2s orbitals of F were kept doubly occupied in the CASSCF calcuations, but only the two sets of 1s orbitals are kept doubly occupied in the MC-QDPT calculations.

The geometry with an Li–F bond length of 3.0 a_0 was taken as the reference geometry to obtain the dominant CSF lists, which are $G_1 = \{\chi_1\}$ and $G_2 = \{\chi_2\}$, where χ_1 is $(4\sigma)^2(5\sigma)^0(1\pi)^4$ and χ_2 is $(4\sigma)^1(5\sigma)^1(1\pi)^4$. No reference orbital is needed, so we used (α_N, α_R, α_T; γ) = (2, 1, 0.5; 0) to determine the CASSCF and MC-QDPT DMOs for the original CASSCF and MC-QDPT diabatization schemes and for the new diabatization scheme in which MC-QDPT wave functions are expressed in terms of CASSCF DMOs.

The adiabatic potential energy curves V_1 and V_2, the diabatic potential energy curves U_{11} and U_{22}, and the diabatic coupling U_{12} obtained by diabatization of CASSCF wave functions with CASSCF DMOs are shown in Figure 1a. The adiabatic potential energy curves have an avoided crossing at large bond length, and the two diabatic potential energy curves (the ionic U_{11} and the covalent U_{22}) cross each other near r_{LiF} = 10.5 a_0, which is much smaller than the experimental [36] distance of 13.7 a_0. The calculated adiabatic potential energy curves and diabatic coupling by diabatization of MC-QDPT wave functions with MC-QDPT DMOs, are shown in Figure 1b. By including dynamical correlation, the diabatic states obtained by MC-QDPT cross at r_{LiF} = 12.5 a_0, which is a significant improvement over CASSCF. The physical reason for the improved performance of the MC-QDPT method is that the electron affinity of fluorine is greatly improved by including dynamical correlation, as is well known from previous work [37].

With our new scheme, we first obtained CASSCF DMOs. Then the adiabatic MC-QDPT wave functions were expressed in terms of the CASSCF DMOs and were used for direct diabatization to obtain the energies of diabatic states and diabatic couplings. The calculated adiabatic and diabatic potential energy curves and diabatic couplings are shown in Figure 1 c. The diabatic states U_{11} and U_{22} calculated by our new scheme with CASSCF DMOs cross at r_{LiF} = 12.5 a_0, which is the same distance as found with the more complicated scheme with MC-QDPT DMOs. Not only do we get a similar crossing distance, we also find that the diabatic potential energy curves calculated with our new scheme are very similar to those calculated by diabatization of MC-QDPT wave function with MC-QDPT DMOs.

3.2. Second test case: Li + HF chemical reaction ($1\ ^2A'$, $2\ ^2A'$)

Along the reaction path of $Li(^2S) + HF(^1\Sigma^+) \rightarrow LiF(^1\Sigma^+) + H(^2S)$ and near to the transition state, the two lowest adiabatic states of LiFH have a strongly avoided crossing [38]. This avoided crossing may be interpreted as the crossing of the valence bond curves corresponding to the reactant bonding configuration and the product bonding configuration. The excited state of the two states involved correlates with $Li(^2P) + HF(^1\Sigma^+)$ in the reactant asymptotic and with $LiF(^3\Sigma^+) + H\ (^2S)$ at the product.

We studied this system with the 6-311G(3df,3pd) basis set [34,35] augmented by diffuse s and p functions with exponents 0.0052 (s) and 0.0097 (p) for Li, 0.089 (s), 0.00001 (s), and 0.083 (p) for F, and 0.037 (s), 0.012 (s), and 0.055 (p) for H. The active space contains the 2s and 2p orbitals of Li, the 2p orbitals of F, and the 1s orbital of H, yielding 7 electrons in 8 orbitals. The 1s orbitals of Li and F atoms and the 2s orbital of F were kept doubly occupied in the CASSCF calcuations, but only the two sets of 1s orbitals are kept doubly occupied in the MC-QDPT calculations.

The potential reference geometries in our calculations were: r_{LiF} = 15.0 a_0 and r_{FH} = 1.73 a_0 in the reactant region and r_{LiF} = 2.96 a_0 and r_{FH} = 15.0 a_0 in the product region with three different Li–F–H angles γ: 45°, 90°, and 135°.

A reference orbital is needed to disentangle the orbital pair $6a'$ and $7a'$, where $6a'$ is the 2s orbital of Li, and $7a'$ is a 2p orbital of Li near reactant asymptote. Since the $6a'$ orbital remains 2s-like along the whole reaction path, but $7a'$ becomes the 1s orbital of H in the product, we chose $6a'$ as the reference orbital, and the MORMO reference geometry was chosen to have the coordinates: r_{LiF} = 15.0 a_0, r_{FH} = 1.73 a_0, and Li–F–H angle equal to 135°.

Next, the dominant CSF lists need to be determined for all reference geometries. For the reactant region we have $G_1 = \{\chi_1\}$ and $G_2 = \{\chi_2\}$, where:

χ_1: $\ldots(4a')^2(5a')^2(6a')^1(7a')^0(1a'')^2$
χ_2: $\ldots(4a')^2(5a')^2(6a')^0(7a')^1(1a'')^2$

where $5a'$ is the $2p_y$ orbital of F (the Li–F axis is the z axis). In the product region we again have $G_2 = \{\chi_2\}$, but—based on the dominant CSFs at all potential reference geometries—we have to add

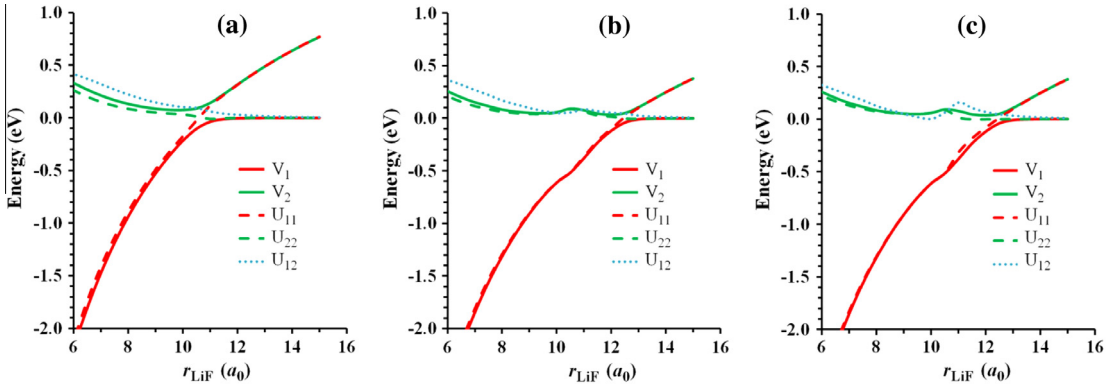

Figure 1. Potential energy curves of the two lowest $^1\Sigma^+$states of LiF. V_1 and V_2 are adiabatic energies; U_{11} and U_{22} are diabatic energies; and U_{12} is the diabatic coupling. We take the zero of energy as the ground-state energy of the dissociation limit. (a) Diabatization with CASSCF DMOs and CASSCF wave functions; (b) diabatization with MC-QDPT DMOs and MC-QDPT wave functions; (c) diabatization with CASSCF DMOs and MC-QDPT wave functions.

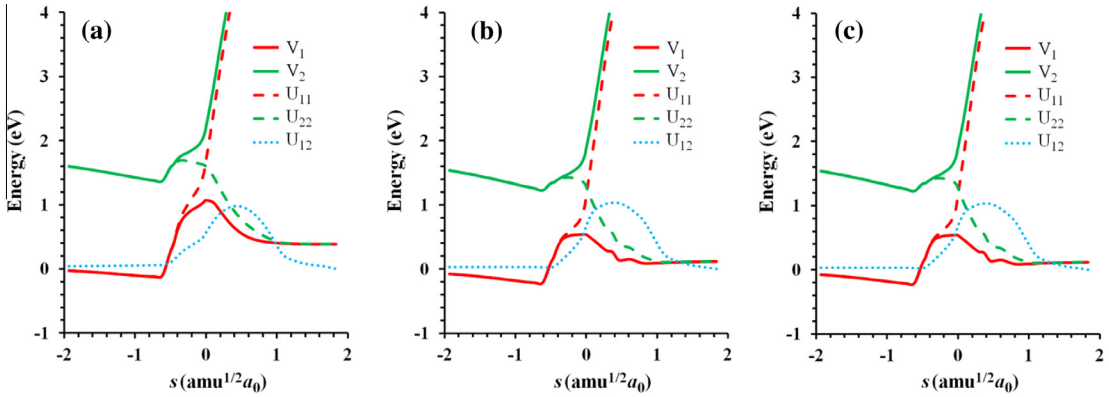

Figure 2. Potential energy curves of the two lowest doublet states of LiFH along the reaction path at a Li–F–H angle γ of 120.0°. We chose the ground state energy of the reactant asymptote, Li(^2S) + HF($^1\Sigma^+$), as the zero reference energy. V_1 and V_2 are adiabatic energies; U_{11} and U_{22} are diabatic energies; and U_{12} is the diabatic coupling. (a) Diabatization with CASSCF DMOs and CASSCF wave functions; (b) diabatization with MC-QDPT DMOs and MC-QDPT wave functions; (c) diabatization with CASSCF DMOs and MC-QDPT wave functions.

two more CSFs to G_1 to provide a good representation in the product region. In particular we add $\{\chi_3^{(1)}\}$, $\{\chi_3^{(2)}\}$ where the spatial parts of the electronic configurations of $\{\chi_3^{(1)}\}$ and $\{\chi_3^{(2)}\}$are the same,

$$\chi_3^{(1)},\ \chi_3^{(2)}:\ \ldots(4a')^2(5a')^1(6a')^1(7a')^1(1a'')^2$$

but they differ in the spin functions.

For the reaction path with $\gamma = 120°$, we performed diabatization with the original CASSCF and MC-QDPT methods as well as with our new scheme. The resulting potential energy curves and diabatic coupling are shown in Figure 2. As the Li atom approach HF molecule, the energy of the ground state decreases slightly along the reaction path, which can be rationalized as noncovalent attraction between Li atom and HF molecule. Then, as the reaction coordinate s approaches -0.6 amu$^{1/2}a_0$, the Li atom gets close to the F atom ($r_{LiF} = 3.68\ a_0$), and the strong HF bond begins to break, so the energy of the ground state increases rapidly. The energy of the ground state further increases as the Li atom continues toward the HF molecule, and finally it decreases after passing the saddle point as the LiF bond is formed. The energy of the ground state near the product asymptotic is higher than that near the reactant asymptote because the HF bond is stronger than the LiF bond.

In Figure 2a, the diabatization is done with CASSCF wave functions, so no dynamical correction is included. The two adiabatic states have a strongly avoided crossing near the transition state, and the two diabatic states cross near $s = 0.03\ a_0$, where s is the distance along the minimum energy path in an isoinertial coordinate system scaled to 1 amu. The barrier height for reaction on the ground-state potential energy surface is about 1.1 eV. With MC-QDPT wave functions, which include dynamical correlation, the adiabatic and diabatic potential energy curves and the diabatic coupling change significantly as compared to Figure 2a, and the barrier height is reduced to about 0.5 eV, as shown in Figure 2 b. With our new method, in which we include the dynamical correlation by MC-QDPT with CASSCF DMOs, the resulting adiabatic and diabatic energies and diabatic coupling agree well with the more complicated diabatization scheme with MC-QDPT DMOs, as shown in Figure 2c.

4. Concluding remarks

The fourfold-way is a direct diabatization method for converting adiabatic electronic wave functions to diabatic ones and computing the diabatic potential energy surfaces and couplings. The key steps are to compute DMOs, to re-express the adiabatic states in terms of DMOs, and to use the re-expressed states to compute the adiabatic-to-diabatic transformation matrix by configurational uniformity. We previously presented algorithms for applying this method to compute both CASSCF diabatic states and MC-QDPT diabatic states. The latter algorithm was based on DMOs determined using the eigenvectors of the effective Hamiltonian that underlies the MC-QDPT calculation. Here we present an algorithm in which the MC-QDPT diabatic states are expressed in terms of the CASSCF DMOs; this simplifies the treatment and, more importantly, it was motivated by our observation that the CASSCF DMOs tend to be smoother than the DMOs that result from the more complicated MC-QDPT procedure. The quality of the diabatic states is not compromised by using the CASSCF DMOs because the new diabatic states still span the same space as the N MC-QDPT adiabatic states that they replace. We illustrate the method on two test cases, the dissociation of LiF and the reaction of Li with HF to yield LiF + H. With the inclusion of dynamical correlation, the results obtained by both the original MC-QDPT diabatization scheme and our new scheme improve over those obtained by the CASSCF diabatization, giving more realistic ionic–covalent crossing distances for LiF and smaller reaction barriers for Li + FH. The results with our new scheme are quite similar to those obtained with the original MC-QDPT diabatization scheme, which is more complicated, validating the new scheme and suggesting that it would be a good choice for nonadiabatic dynamics studies in the future.

Acknowledgments

This work was supported in part by the U.S. Department of Energy, Office of Basic Energy Sciences, under SciDAC Grant No. DE-SC0008666.

References

[1] M.S. Child, in: R.B. Bernstein (Ed.), Atom-Molecule Collision Theory, Plenum, New York, 1979, pp. 427–465.
[2] A.W. Jasper, B.K. Kendrick, C.A. Mead, D.G. Truhlar, in: X. Yang, K. Liu (Eds.), Modern Trends in Chemical Reaction Dynamics, World Scientific, Singapore, 2003, pp. 329–391.
[3] C.A. Mead, D.G. Truhlar, J. Chem. Phys. 77 (1982) 6090.
[4] H. Nakamura, D.G. Truhlar, J. Chem. Phys. 115 (2001) 10353.
[5] H. Nakamura, D.G. Truhlar, J. Chem. Phys. 117 (2002) 5576.
[6] H. Nakamura, D.G. Truhlar, J. Chem. Phys. 118 (2003) 6816.
[7] S. Nangia, D.G. Truhlar, J. Chem. Phys. 124 (2006) 124309.
[8] Z.H. Li, R. Valero, D.G. Truhlar, Theor. Chem. Acc. 118 (2007) 9.
[9] D. Bonhommeau, D.G. Truhlar, J. Chem. Phys. 129 (2008) 14302.
[10] D. Bonhommeau, R. Valero, D.G. Truhlar, A. Jasper, J. Chem. Phys. 130 (2009) 234303.
[11] R. Valero, D.G. Truhlar, J. Chem. Phys. 125 (2006) 194305.
[12] R. Valero, D.G. Truhlar, A.W. Jasper, J. Phys. Chem. A 112 (2008) 5756.
[13] R. Valero, D.G. Truhlar, J. Chem. Phys. 137 (2012) 22A539.
[14] P. Siegbahn, A. Heiberg, B.O. Roos, B.A. Levy, Phys. Scripta 21 (1980) 323.
[15] B.O. Roos, P.R. Taylor, P.E.M. Siegbahn, Chem. Phys. 48 (1980) 157.

[16] K. Ruedenberg, M.W. Schmidt, G.M. Gilbert, S.T. Elbert, Chem. Phys. 71 (1982) 41.
[17] H. Nakano, J. Chem. Phys. 99 (1993) 7983.
[18] H. Nakano, Chem. Phys. Lett. 207 (1993) 372.
[19] J. Finley, P.-Å. Malmqvist, B.O. Roos, L. Serrano-Andrés, Chem. Phys. Lett. 288 (1998) 299.
[20] K. Andersson, P.-Å. Malmqvist, B.O. Roos, A.J. Sadlej, K. Wolinski, J. Phys. Chem. 94 (1990) 5488.
[21] K. Andersson, P.-Å. Malmqvist, B.O. Roos, J. Chem. Phys. 96 (1992) 1218.
[22] K. Hirao, Chem. Phys. Lett. 190 (1992) 374.
[23] P.M. Kozlowski, E.R. Davidson, Chem. Phys. Lett. 222 (1994) 615.
[24] N. I. Gidopoulos, E. K. U. Gross, arXiv:cond-mat/0502433.
[25] A. Granovsky, J. Chem. Phys. 134 (2011) 214113.
[26] T. Shiozaki, W. Győrffy, P. Celani, H.-J. Werner, J. Chem. Phys. 135 (2011) 81106.
[27] C. Woywod, W. Domcke, A.L. Sobolewski, H.-J. Werner, J. Chem. Phys. 100 (1994) 1400.
[28] M.S. Topaler, D.G. Truhlar, X.Y. Chang, P. Piecuch, J.C. Polanyi, J. Chem. Phys. 108 (1998) 5349.
[29] H. Lischka, M. Dallos, P.G. Szalay, D.R. Yarkony, R. Shepard, J. Chem. Phys. 120 (2004) 7322.
[30] G.J. Atchity, K. Ruedenberg, Theor. Chem. Acc. 97 (1997) 47.
[31] L.R. Kahn, P.J. Hay, I. Shavitt, J. Chem. Phys. 61 (1974) 3530.
[32] H. Nakamura, J. D. Xidos, et al., HONDOPLUS-v5.2, based on HONDO–v99.6, University of Minnesota, Minneapolis, MN, 2013.
[33] HONDO 99.6, by M. Dupuis, A. Marquez, E. R. Davidson, 1999, based on HONDO 95.3, by M. Dupuis, A. Marquez, E. R. Davidson, Quantum Chemistry Program Exchange (QCPE), Indiana University, Bloomington, IN.
[34] R. Krishnan, J.S. Binkley, R. Seeger, J.A. Pople, J. Chem. Phys. 72 (1980) 650.
[35] M.J. Frisch, J.A. Pople, J.S. Binkley, J. Chem. Phys. 80 (1983) 3265.
[36] R. Grice, D.R. Herschbach, Mol. Phys. 27 (1974) 159.
[37] F. Sasaki, M. Yoshimine, Phys. Rev. A 9 (1974) 26.
[38] A.W. Jasper, M.D. Hack, D.G. Truhlar, P. Piecuch, J. Chem. Phys. 116 (2002) 8353.